Comput. Methods Appl. Mech. Engrg. 199 (2010) 723–733

Contents lists available at ScienceDirect

Comput. Methods Appl. Mech. Engrg.

journal homepage: www.elsevier.com/locate/cma

Partitioned formulation of internal and gravity waves interacting with flexible structures

K.C. Park [a,b,*], R. Ohayon [c], C.A. Felippa [b], J.A. González [d]

[a] Division of Ocean Systems Engineering, School of Mechanical Engineering, KAIST, Daejeon 305-701, Republic of Korea
[b] Department of Aerospace Engineering Sciences, University of Colorado at Boulder, CO 80309-429, USA
[c] Chair of Mechanics, Structural Mechanics and Coupled System Laboratory, Conservatoire National des Arts et Métiers (CNAM), 75003 Paris, France
[d] Departamento de Ingeniería del Diseño, Escuela Técnica Superior de Ingenieros, Camino de los Descubrimientos s/n, 41092 Sevilla, Spain

ARTICLE INFO

Article history:
Received 12 July 2009
Received in revised form 4 October 2009
Accepted 5 November 2009
Available online 12 November 2009

Keywords:
Internal acoustic and gravity waves
Fluid–structure interaction
Partitioned FSI formulation

ABSTRACT

This paper presents a partitioned modeling of internal and gravity fluid waves that interact with flexible structures. The governing interaction model consists of three completely partitioned entities: fluid model, structural model, and interface model that acts as an internal constraint on the fluid–structure interface boundary. Thus, the proposed partitioned multi-physics modeling can employ two completely modular fluid and structure software modules plus an interface solver, hence amenable to partitioned solution algorithms. The interface discretization can exploit the nonmatching interface algorithm previously developed via the method of localized Lagrange multipliers. Also noted is that the present fluid model can make use of widely available finite element software for standard Poisson-type problems.

1. Introduction

Fluid–structure interaction (FSI) phenomena have recently emerged as one of the most widely encountered multi-physics problems in science and engineering. As a result, various specialized FSI formulations have been developed and successfully applied to problems involving internal fluid problems [1–22], external fluids problems [23–40], and recently biomechanics [41–46], among others. Interested readers may consult a review by Dowell and Hall [47] for general FSI problems viewed from the fluid mechanics context, by Tijsseling [48] for piping flow, and by de Boera et al. [49] for various interface coupling methods. From the viewpoint of formulation, modeling, discretization and numerical solution, a wide range of computational procedures have been developed over the past three decades. They range from tightly-to-loosely coupled to locally partitioned [51–70]. For example, FSI problems of blood flow typically adopt tightly coupled formulation and solution procedures [41], whereas aeroelasticity problems employ partitioned solution procedures [71]. The view of present authors is that, as much as possible, the task for multi-physics simulation is facilitated by adopting partitioned solution procedures. Among the beneficial sides of invoking partitioned solution procedures, we mention substantial reductions, both in development time and cost, of the development of single-discipline oriented analysis software, upgrading ease and simplified maintenance, and the efficient use of discipline-specific specialists.

This has motivated us to undertake a series of critical revision of FSI problems and, if necessary and/or possible, to reformulate FSI problems such that the resulting form may facilitate the treatment of partitioned solution procedures. Because of our background and experience, we begin with the reformulation of a flexible structure interacting with internal compressive fluids including gravity effects while deferring reformulations of other FSI problems to a later exposition. It should be pointed out that we focus solely on FSI formulations with small displacements and the method of localized Lagrange multipliers, although not necessarily restricted to linear, that leads naturally to partitioned solution procedures for the remainder of the paper. Readers interested in other formulations such as Eulerian–Lagrangian approach, fictitious/mortar element approach may consult recent articles [70,66,61] and references therein. To this end, we offer a review of existing FSI formulations of internal waves with gravity and free surface interacting with flexible structures.

The governing equations of motion for inviscid internal fluids contained by flexible structures often rely on the so-called excess pressure [75] or modified pressure in [76] defined as follows: "if the absolute pressure occurs in the boundary conditions, as happens if part of the boundary is an interface with another fluids or if it is a free surface, ...the effect of gravity reenters the problem." Thus, the modified pressure is the difference between the total pressure and the gravity-induced pressure. This concept is

* Corresponding author. Address: Division of Ocean Systems Engineering, School of Mechanical Engineering, KAIST, Daejeon 305-701, Republic of Korea.
E-mail addresses: k.c.park@kaist.ac.kr, kcpark@colorado.edu (K.C. Park).

0045-7825/$ - see front matter © 2009 Elsevier B.V. All rights reserved.
doi:10.1016/j.cma.2009.11.005

adequate for air whose boundary condition involves only the velocity. When the fluids interact with flexible structures, however, complications arise depending on how the interface kinematic compatibility condition is enforced. For example, Morand and Ohayon [13] utilize the modified pressure. To compensate for the omission of the fluid pressure due to gravity, they embed the fluid pressure into the initial stress in the governing equations of motion for structures. Hence, the structural analysis software must have access to the current fluid field geometry that is in turn used to compute the initial stress acting on the fluid–structure interface. This requirement hinders the use of partitioned analysis. There is an additional complication in prescribing the interface compatibility conditions, viz., the enforcement of the fluid–structure interface conditions in terms of the modified pressure instead of the total pressure as a conjugate Lagrange multiplier may lead to an inconsistent formulation or involve an iterative strategy.

The present formulation reverts to the total pressure for the construction of fluid energy, and employs the localized Lagrange multipliers [50,57–59,63] for treating the interaction. These two choices render unnecessary the incorporation of gravity-induced pressure as initial stress in the equations of motion for structures, and lead to a consistent construction of interface kinematic compatibility. Conditioning of the interface compatibility is achieved by a regularization of the localized Lagrange multipliers [59,18]. It will be shown that the resulting reformulation enables one to employ two stand-alone software modules, viz., a structural analyzer and an internal acoustic and gravity wave model for conducting the coupled dynamics of internal and gravity waves interacting with flexible structures. In so doing, we restrict ourselves in the present paper to the partitioned formulation aspects of internal fluid–structure interaction and leave computer implementation aspects to a later article, although we include a summary of interface treatment strategies. The rest of the paper is organized as follows.

Section 2 reviews the method of classical Lagrange multipliers to enforce the fluid–structure interface constraint, and then moves on to describe the method of localized Lagrange multipliers. A distinct feature of the latter method introduces two linearly independent Lagrange multipliers, one for the fluid partition boundary and the other for the structural partition boundary. This enables to enforce the force and moment balance across the interface boundary for nonmatching discretizations. Thus, the fluid and structural meshes can be chosen independently without having to introduce a special remeshing or interpolations of the classical Lagrange multipliers.

Section 3 derives inviscid fluid equations that model coupled acoustic pressure and gravity pressure as well as nonlinearities by treating the acoustic and gravity pressure terms as initial stresses. This formalism adopts the same finite element discretization techniques used in structural modeling. More precisely, the internal variational energy density term $\boldsymbol{\sigma}_f : \nabla\delta\mathbf{u}_f$ is discretized instead of $(\nabla\cdot\boldsymbol{\sigma}_f)\cdot\delta\mathbf{u}_f$ that often employed existing literature(see, e.g., [13]).

Section 4 outlines a general derivation of the variational equation of motion for structures and specializes to a linearized equation with initial stress that produces the well-known geometric stiffness.

Section 5 discusses the discretization of the fluid–structure interface constraint functional, of the virtual work of the fluid partition and of the structural partition. The stationarity of the total variational expressions, viz., the discretized constraint functional, the discretized virtual work of the fluid and structure partitions, leads to the present partitioned coupled fluid–structure interaction model, which can be used for vibration analysis as well as transient response analysis.

Section 6 presents the partitioned equation for vibration analysis, an implicit–implicit transient response analysis algorithm, an implicit–explicit algorithm, and an explicit–explicit algorithm. It is shown that the three transient analysis algorithms can be implemented within one software module as their differences are in how the stiffness force terms are treated.

Section 7 discusses the applicability and limitations of the present FSI formulation as well as further work to be carried out in order to extend the present work to couple with external acoustics and surface wave motions.

2. Overview of present partitioned FSI formulation

The essence of the present partitioned formulation is stated as

$$\delta\Pi_f + \delta\Pi_s + \delta\pi_\ell = 0, \tag{1}$$

where $\delta\Pi_f$ is the virtual work for the fluid; $\delta\Pi_s$ is the virtual work for the flexible structure; and, $\delta\pi_\ell$ is the partition interface constraint, respectively. It should be noted that $\delta\Pi_f = 0$ yields the governing equations of motion for the fluid. Similarly, $\delta\Pi_s = 0$ yields the equations of motion for the structure. This implies that the present formulation may utilize two independently developed fluid and flexible structural dynamics analysis software modules to perform FSI analysis, with the addition of an interface treatment module whose main function is to enforce the interface constraint $\delta\pi_\ell = 0$.

We now describe the formulation of each of the three virtual work expressions in the subsequent sections.

3. Fluid–structure interface description

We adopt the viewpoint that the interface between fluid and structure strictly as *internal constraints*. This viewpoint obviates the need for evaluating the interface *boundary* energy terms for the fluid and structure. More specifically, the fluid–structure interface materializes on account of distinctly different constitutive relations for the two media. We then treat the internal interface via the method of *localized* Lagrange multipliers that, as subsequently demonstrated, leads naturally to a partitioned formulation.

We start by reviewing the interface conditions (cf. see [13]). The interface compatibility condition for infinitely small displacements may be stated as (see Fig. 1)

$$c_{fs} = (\mathbf{u}_f - \mathbf{u}_s)\cdot\mathbf{n} = 0, \tag{2}$$

where $(\mathbf{u}_f, \mathbf{u}_s)$ are the fluid and structural displacement, respectively, and $\mathbf{n}$ is the unit normal to the interface surface.

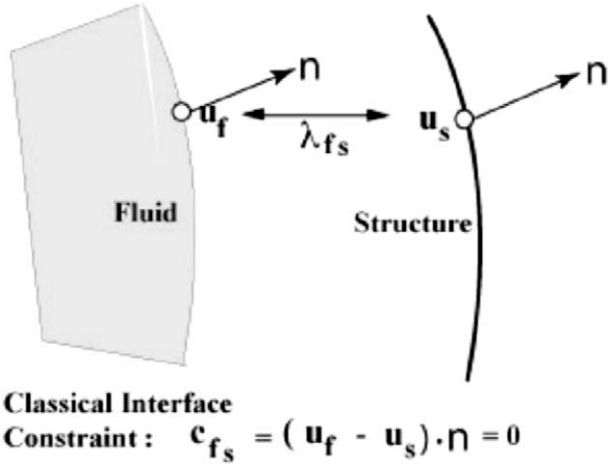

Fig. 1. Classical treatment of the partition interface frame.

Enforcement of the above interface constraint is realized by the classical Lagrange multipliers method, resulting in a functional form

$$\pi_c = \int_{\Gamma_{int}} \lambda_{fs} c_{fs}\, dS. \tag{3}$$

In passing, it should be noted that in most existing formulations [13,77,78] the fluctuation pressure on the boundary is used to form the interface constraint functional

$$\pi_{con} = \int_{\Gamma_{int}} p_e c_{fs}\, dS, \tag{4}$$

for which p_e denotes the fluctuation pressure, and the displacements $(\mathbf{u}_f, \mathbf{u}_s)$ are to be interpreted as perturbation quantities, not the total fluid and structural displacements.

In the present work we introduce a localized partition or *frame* as shown in Fig. 2. As a consequence, fluid and structure do not interact directly but with the reference interface. This may be expressed as

$$\begin{aligned} &\text{Fluid interface constraint}: \mathbf{c}_f = (\mathbf{u}_f - \mathbf{u}_b)\cdot\mathbf{n} = 0,\\ &\text{Structure interface constraint}: \mathbf{c}_s = (\mathbf{u}_s - \mathbf{u}_b)\cdot\mathbf{n} = 0, \end{aligned} \tag{5}$$

where $\mathbf{u}_b$ is the *frame* displacement treated as an independent displacement variable. It will be shown that the interface forces and moment balance equations are obtained with respect to this frame displacement, a feature that can be exploited both for solution regularization and software modularity. The resulting constraint functional thus requires two independent Lagrange multipliers (see Fig. 3):

$$\pi_\ell(\mathbf{u}_f, \mathbf{u}_s, \mathbf{u}_b, \boldsymbol{\lambda}_f, \boldsymbol{\lambda}_s) = \int_{S_f} \boldsymbol{\lambda}_f^T \mathbf{c}_f\, dS + \int_{S_s} \boldsymbol{\lambda}_s^T \mathbf{c}_s\, dS. \tag{6}$$

The first variation of the fluid–structure interface constraint involves five variables:

$$\begin{aligned} \delta\pi_\ell(\mathbf{u}_f, \mathbf{u}_s, \mathbf{u}_b, \boldsymbol{\lambda}_f, \boldsymbol{\lambda}_s) = &+ \int_{S_f} \delta\boldsymbol{\lambda}_f^T (\mathbf{u}_f - \mathbf{u}_b)\cdot\mathbf{n}\, dS + \int_{S_s} \delta\boldsymbol{\lambda}_s^T (\mathbf{u}_s - \mathbf{u}_b)\cdot\mathbf{n}\, dS\\ &+ \int_{S_f} \boldsymbol{\lambda}_f^T \delta\mathbf{u}_f\cdot\mathbf{n}\, dS + \int_{S_s} \boldsymbol{\lambda}_s^T \delta\mathbf{u}_s\cdot\mathbf{n}\, dS\\ &- \int_{S_f} (\boldsymbol{\lambda}_f^T + \boldsymbol{\lambda}_s^T)\delta\mathbf{u}_b\cdot\mathbf{n}\, dS. \end{aligned} \tag{7}$$

If the interface geometry is allowed to vary, the following terms must be added as discussed in [13,77]:

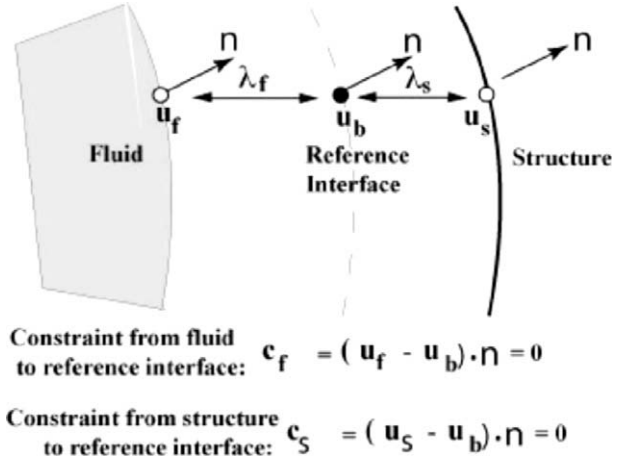

Fig. 2. Localized treatment of the partition interface frame.

$$\begin{aligned} \frac{\partial\pi_\ell}{\partial\mathbf{n}}\delta\mathbf{n} = &\int_{S_f} \boldsymbol{\lambda}_f^T(\mathbf{u}_f - \mathbf{u}_b)\cdot\delta\mathbf{n}\, dS + \int_{S_s} \boldsymbol{\lambda}_s^T(\mathbf{u}_s - \mathbf{u}_b)\cdot\delta\mathbf{n}\, dS\\ &\text{in which } \delta\mathbf{n} = \frac{\partial\mathbf{n}}{\partial\mathbf{u}}\delta\mathbf{u}. \end{aligned} \tag{8}$$

In the present paper we will replace $\mathbf{n}$ by an averaged value for each discrete interface segment or interface element, $\mathbf{n}_{av}$. This normal is not subject to variation. Consequently, (7) becomes

$$\begin{aligned} \delta\pi_\ell(\mathbf{u}_f, \mathbf{u}_s, \mathbf{u}_b, \boldsymbol{\lambda}_f, \boldsymbol{\lambda}_s) = &+ \int_{S_f} \delta\boldsymbol{\lambda}_f^T(\mathbf{u}_f - \mathbf{u}_b)\cdot\mathbf{n}_{av}\, dS + \int_{S_s} \delta\boldsymbol{\lambda}_s^T(\mathbf{u}_s - \mathbf{u}_b)\cdot\mathbf{n}_{av}\, dS\\ &+ \int_{S_f} \boldsymbol{\lambda}_f^T\delta\mathbf{u}_f\cdot\mathbf{n}_{av}\, dS + \int_{S_s} \boldsymbol{\lambda}_s^T\delta\mathbf{u}_s\cdot\mathbf{n}_{av}\, dS\\ &- \int_{S_f} (\boldsymbol{\lambda}_f^T + \boldsymbol{\lambda}_s^T)\delta\mathbf{u}_b\cdot\mathbf{n}_{av}\, dS. \end{aligned} \tag{9}$$

The preceding variational functional constitutes one of the three variational expressions for the derivation of the partitioned fluid–structure interaction equation set. The remaining two are the virtual work of the fluid domain and that of the flexible structure domain. Their derivations are discussed in the subsequent sections.

4. Variational formulation of internal acoustics and gravity waves

4.1. Virtual work for fluid

The formulation of internal and gravity fluid waves have been studied by many investigators [73,72,75,13], among others. For the present purpose, we will assume the flow to be inviscid and begin with the following Lagrangian virtual work principle stated over the fluid volume V_f:

$$\begin{aligned} \delta\Pi_f = &\int_{V_f} \{\nabla_0\cdot\mathbf{T} + \mathbf{b}_0 - \rho_0\ddot{\mathbf{u}}_f\}\cdot\delta\mathbf{u}_f\, dV_0 = 0, \quad \mathbf{T} = J\,\mathbf{F}^{-1}\cdot\boldsymbol{\sigma},\\ &\mathbf{F} = \nabla\mathbf{x}_f = \mathbf{I} + \nabla\mathbf{u}_f, \quad \mathbf{x}_f = \mathbf{X} + \mathbf{u}_f, \quad \mathbf{X} = X\mathbf{i} + Y\mathbf{j} + Z\mathbf{k},\\ &\mathbf{u}_f = u_1\mathbf{i} + u_2\mathbf{j} + u_3\mathbf{k} = u\mathbf{i} + v\mathbf{j} + w\mathbf{k},\\ &\nabla_0 = \frac{\partial}{\partial X}\mathbf{i} + \frac{\partial}{\partial Y}\mathbf{j} + \frac{\partial}{\partial Z}\mathbf{k}, \quad J = \det(\mathbf{F}) \approx 1 + \nabla\cdot\mathbf{u}_f. \end{aligned} \tag{10}$$

In the above variational equation, we assume that both the prescribed traction and displacement boundary conditions are exactly satisfied; $\mathbf{T}$ and $\boldsymbol{\sigma}$ are the first Piola–Kirchhoff stress and the Cauchy stress tensor, respectively; $\mathbf{b}_0$ is the body force; ρ_0 is the mass density; $\ddot{\mathbf{u}}_f$ is the fluid particle acceleration; $\mathbf{X}$ and $\mathbf{u}_f$ refer to the initial configuration and the fluid displacement, respectively; and subscript 0 denotes the initial configuration. In the above variational form, we omitted the convective term and the viscosity term from the standard Navier-Stokes equations for the fluid as usually the case with modeling of internal waves.

As we will see shortly, the starting variational equations both for the fluid $(10)_1$ and for the structure are the same. It is in the use of constitutive relations that will lead to fluid or solid model. In the present study we take the fluid stress tensor as modeled by

$$\begin{aligned} &\boldsymbol{\sigma} = -P\mathbf{I}_3, \quad P = p_{ac} + p_{gr}, \quad p_{ac} = -\rho_0(z)c^2\nabla\cdot\mathbf{u}_f,\\ &p_{gr} = \rho(z)g(h - z), \quad z = Z + \mathbf{k}\cdot\mathbf{u}_f, \end{aligned} \tag{11}$$

where $\mathbf{I}_3$ is the (3×3) identity matrix; P is the total pressure; p_{ac} is known as the fluctuation pressure that causes acoustic waves; p_{gr} is the pressure due to gravity that causes gravity waves; p_a is the atmospheric pressure; c is the speed of sound of the fluid; h is the depth of the fluid measured from the free surface to the bottom of the fluid that is taken as the origin of the Z-coordinate, sometimes referred to as hydraulic head; z is the vertical coordinate at the fluid particle of interest; $\mathbf{u}_f$ is the particle displacement; g is

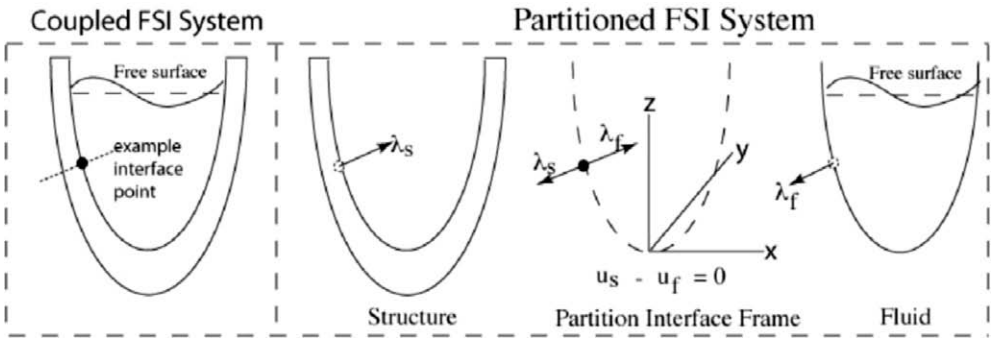

Fig. 3. Partitioning of internal fluid–structure interaction system.

the gravitational acceleration; and $\mathbf{k}$ is the upward unit vector along the vertical direction, that is, the Z-direction.

It is emphasized that, in contrast to [13], both p_{ac} and p_{gr} are expressed in a Lagrangian frame. A first-order expansion of the first Piola-Kirchhoff stress tensor $\mathbf{T}$ gives:

$$\begin{aligned}\mathbf{T} &\approx -(1+\nabla\cdot\mathbf{u}_f)P\mathbf{I}_3 + P(\nabla\mathbf{u}_f)\\ &\approx -(1+\nabla\cdot\mathbf{u}_f)P\mathbf{I}_3 + P(\mathrm{diag}[\nabla\mathbf{u}_f]),\end{aligned} \tag{12}$$

where the replacement of $(\nabla\mathbf{u}_f)^T$ by $\mathrm{diag}[(\nabla\mathbf{u}_f)^T]$ is effected by inviscid assumption in which case fluid experiences no resistance to shearing strains.

At this juncture it should be mentioned that there are two paths by which one can carry out variational process and subsequently discretize the resulting variational equation to obtain the discrete equations of motion. One is to obtain $\nabla\cdot\mathbf{T}$ and substitute into $(10)_1$. Then carry out integration by part only for terms involving ∇p_{ac}. This is the path taken in [77,78]. In the present paper, we proceed along the lines of solid mechanics and the integration by parts to arrive at the virtual energy density for fluid that is analogous to the term $(\boldsymbol{\sigma}:\boldsymbol{\epsilon})$ used for finite element discretization in solid mechanics. To this end, by using the formula

$$(\nabla_0\cdot\mathbf{T})\cdot\delta\mathbf{u} = \nabla\cdot(\mathbf{T}\cdot\delta\mathbf{u}) - \mathbf{T}^T:\nabla_0\delta\mathbf{u}, \tag{13}$$

the first term in $(10)_1$ is transformed to

$$\int_{V_0}(\nabla_0\cdot\mathbf{T})\cdot\delta\mathbf{u}_f\,dV_0 = \int_{\Gamma}(\mathbf{T}\cdot\delta\mathbf{u}_f)_i\cdot\mathbf{n}_i\,d\Gamma_i - \int_{V_0}\mathbf{T}^T:\nabla_0\delta\mathbf{u}_f\,dV_0. \tag{14}$$

In the above equation, the first free surface integral represents surface traction energy while the second one is the internal energy. As noted in the beginning of Section 2, we treat the fluid–structure interface as *internal constraint*, not as a boundary condition for the fluid. This is another contrast with classical fluid formulations that treat the fluid surface contacting the structure by a wall boundary condition.

4.2. Surface energy model

On the free surface we have

$$P = p_a + \sigma_s\nabla\cdot\mathbf{n} = p_a + \rho_0 g\mathbf{k}\cdot\mathbf{u}_f, \tag{15}$$

where p_a the atmospheric pressure acting on the surface of the fluid; σ_s represents the surface tension (for water $\sigma_s\approx 70$ dynes/cm); and the well-known Young–Laplace equation that relates the surface tension to the gravity force is used. It should be noted that the preceding model is valid in principle for flat surfaces. As the surface of each discretized surface element may be assumed to be flat even though the overall surface may be curved, we are permitted to employ the flat surface hypothesis. Substituting the above relation into the first of (14) leads to

$$\int_{\Gamma_f}(\mathbf{T}\cdot\delta\mathbf{u}_f)\cdot\mathbf{n}d\Gamma = -\int_{\Gamma_f}p_a(\mathbf{n}\cdot\delta\mathbf{u}_f)\,d\Gamma - \int_{\Gamma_f}\rho_0 g(\mathbf{k}\cdot\mathbf{u}_f)(\mathbf{n}\cdot\delta\mathbf{u}_f)\,d\Gamma. \tag{16}$$

It should be noted that the present surface tension energy does not account for surface curvature effects as detailed in Landau [74] and Lighthill [75]. However, its effect is known to be within a few percentage error for waves whose length exceeds 0.1 m.

4.3. Internal energy model

Inserting the constitutive relation (11) into the stress tensor (12) gives

$$\mathbf{T}^T = -(1+\nabla\cdot\mathbf{u}_f)(-\rho_0 c^2\nabla\cdot\mathbf{u}_f + p_{gr})\mathbf{I}_3 + (p_{ac}+p_{gr})\mathrm{diag}(\nabla\mathbf{u}_f). \tag{17}$$

The internal fluid energy density $(\mathbf{T}^T:\nabla\delta\mathbf{u}_f)$ is thus obtained as

$$\begin{aligned}\mathbf{T}^T:\nabla\delta\mathbf{u}_f = &-(1+\nabla\cdot\mathbf{u}_f)(-\rho_0 c^2\nabla\cdot\mathbf{u}_f + p_{gr})\nabla\cdot\delta\mathbf{u}_f\\ &+(p_{ac}+p_{gr})\sum_{i=1}^{3}\frac{\partial u_i}{\partial X_i}\cdot\frac{\partial\delta u_i}{\partial X_i}\end{aligned} \tag{18}$$

$$p_{gr} = \rho_0 g(h - Z - \mathbf{u}_f\cdot\mathbf{k}), \quad p_{ac} = -\rho_0 c^2\nabla\cdot\mathbf{u}_f.$$

The internal energy is thus obtained by integrating over the fluid volume as

$$\begin{aligned}&\int_{V_f}\mathbf{T}^T:\nabla\delta\mathbf{u}_f\,dV\\ &\quad= \int_{V_f}(\nabla\cdot\mathbf{u}_f)(\rho_0 c^2)(\nabla\cdot\delta\mathbf{u}_f)\,dV - \int_{V_f}p_{gr}(\nabla\cdot\delta\mathbf{u}_f)\,dV\\ &\quad\quad- \int_{V_f}(\nabla\cdot\mathbf{u}_f)(p_{gr})(\nabla\cdot\delta\mathbf{u}_f)\,dV + \int_{V_f}\sum_{i=1}^{3}\left(\frac{\partial u_i}{\partial X_i}\right)(p_{gr})\left(\frac{\partial\delta u_i}{\partial X_i}\right)dV\\ &\quad\quad- \int_{V_f}(\nabla\cdot\mathbf{u}_f)(p_{ac})(\nabla\cdot\delta\mathbf{u}_f)\,dV\\ &\quad\quad+ \int_{V_f}\sum_{i=1}^{3}\left(\frac{\partial u_i}{\partial X_i}\right)(p_{ac})\left(\frac{\partial\delta u_i}{\partial X_i}\right)dV.\end{aligned} \tag{19}$$

4.4. Density stratified fluids

If the fluid density $\rho(z)$ varies along the z-axis, the second term in the foregoing equation becomes

$$\int_{V_f} p_{gr}\nabla\cdot\delta\mathbf{u}_f\,dV = \int_{S_f} p_{gr}\mathbf{k}\cdot\delta\mathbf{u}_f\,dS - \int_{V_f}\nabla p_{gr}\cdot\delta\mathbf{u}_f\,dV$$
$$= -\int_{V_f}\nabla p_{gr}\cdot\delta\mathbf{u}_f\,dV, \tag{20}$$

where $p_{gr}=0$ is used on the free surface in the first term of $(20)_1$. While we defer the problem of density stratification due to gravity to a subsequent work, the second terms in $(19)_2$, when the density varies due solely to gravity, requires the following modifications.

First, for ease of derivation we employ a change of variable to express the pressure due to gravity as

$$p_{gr} = \rho g(Z'+\xi), \quad Z' = h - Z, \quad \xi = -(\mathbf{u}_f\cdot\mathbf{k}). \tag{21}$$

That is, Z' is measured from the free surface to the fluid particle, and ξ is a small displacement of the particle toward the bottom of the container. Using the change of variables, $\nabla_{Z'}p_{gr}$ is evaluated as

$$\nabla_{Z'}p_{gr} = \frac{\partial p_{gr}}{\partial Z'}\mathbf{k}' = \left\{\frac{\partial\rho}{\partial Z'}g(Z'+\xi)+\rho g+\frac{\partial\xi}{\partial Z'}\right\}\mathbf{k}',$$
$$\mathbf{k}' = -\mathbf{k} \approx \left\{\frac{\partial\rho}{\partial Z'}g(Z'+\xi)+\rho g\right\}\mathbf{k}'. \tag{22}$$

Second, one must employ the constitutive relation for density that reflects the effect of gravity influence, viz.,

$$\rho(z) = \rho_0 + \frac{\partial p_{gr}}{\partial Z'}\cdot\frac{\partial\rho_0}{\partial p}\xi = \rho_0 + (\rho_0 g)\cdot\left(\frac{1}{c^2(z)}\right)\xi, \quad \frac{\partial\rho_0}{\partial p} = \frac{1}{c^2(z)}. \tag{23}$$

Substituting (22) and (23) into (20), one obtains

$$\int_{V_f} p_{gr}\nabla\cdot\delta\mathbf{u}_f\,dV = -\int_{V_f}\rho_0\left[1-\frac{\rho_0'(z)}{\rho_0(z)}Z'\right](\mathbf{g}\cdot\delta\mathbf{u}_f)\,dV$$
$$-\frac{1}{2}\int_{V_f}\rho_0(z)[N]^2\delta(\mathbf{k}\cdot\mathbf{u}_f)]^2\,dV[N]^2$$
$$= -\left[\frac{g^2}{c^2(z)}+g\frac{\rho_0'}{\rho_0}\right], \quad \rho' = \frac{\partial\rho}{\partial Z} = -\frac{\partial\rho}{\partial Z'}. \tag{24}$$

Here $[N]$ is referred to as the Väisälä-Brunt frequency and $[N]^2$ represents the maximum stiffness solely due to gravity. Readers interested in a classical derivation of the foregoing stiffness may consult Chapter 4 of Lighthill [75].

4.5. External energy

The external force $\mathbf{b}_0$ consists of two parts: the gravity force $(\rho_0\mathbf{g})$ and any externally excited forces such as an acoustically generated wave generator $\mathbf{f}_f(t)$. Thus, the virtual external work may be expressed as

$$\int_{V_f}\mathbf{b}_0\cdot\delta\mathbf{u}_f dV = \int_{V_f}\{\rho_0\mathbf{g}\cdot\delta\mathbf{u}_f + \mathbf{f}_f(t)\cdot\delta\mathbf{u}_f\}dV. \tag{25}$$

4.6. Partitioned variational equation for fluids

Substituting (14), (16), (19), (24), and (25) into $(10)_1$ the partitioned variational equation for fluids is finally obtained as shown below:

$$\text{Inertia force}: \int_{V_f}\rho_0\ddot{\mathbf{u}}\cdot\delta\mathbf{u}_f\,dV,$$
$$\text{Acoustic stiffness}: +\int_{V_f}(\nabla\cdot\mathbf{u}_f)(\rho_0c^2)(\nabla\cdot\delta\mathbf{u}_f)\,dV,$$
$$\text{Väisälä-Brunt stiffness}: +\frac{1}{2}\int_{V_f}\rho_0(z)[N]^2\delta(\mathbf{k}\cdot\mathbf{u}_f)]^2\,dV,$$
$$\text{Gravity geometric stiffness 1}: -\int_{V_f}(\nabla\cdot\mathbf{u}_f)(p_{gr})(\nabla\cdot\delta\mathbf{u}_f)\,dV,$$
$$\text{Gravity geometric stiffness 2}: +\int_{V_f}\sum_{i=1}^{3}\left(\frac{\partial u_i}{\partial X_i}\right)(p_{gr})\left(\frac{\partial\delta u_i}{\partial X_i}\right)dV,$$
$$\text{Acoustic geometric stiffness 1}: -\int_{V_f}(\nabla\cdot\mathbf{u}_f)(p_{ac})(\nabla\cdot\delta\mathbf{u}_f)\,dV,$$
$$\text{Acoustic geometric stiffness 2}: +\int_{V_f}\sum_{i=1}^{3}\left(\frac{\partial u_i}{\partial X_i}\right)(p_{ac})\left(\frac{\partial\delta u_i}{\partial X_i}\right)dV,$$
$$\text{Surface stiffness}: +\int_{S_f}\rho_0 g(\mathbf{k}\cdot\mathbf{u}_f)(\mathbf{k}\cdot\delta\mathbf{u}_f)\,dS,$$
$$\text{Body force}: =\int_{V_f}\mathbf{f}(t)\cdot\delta\mathbf{u}_f\,dV,$$
$$\text{Atmospheric pressure}: -\int_{S_f}p_a\mathbf{n}\cdot\delta\mathbf{u}_f dS,$$
$$\text{Density stratification}: +\int_{V_f}\rho_0' gZ'(\mathbf{k}\cdot\delta\mathbf{u}_f)\,dV,$$
$$\text{Väisälä-Brunt frequency}: [N] = \sqrt{-\frac{g^2}{c^2(z)}-g\frac{\rho_0'}{\rho_0}}, \tag{26}$$

where the pressure due to gravity p_{gr} and the acoustic pressure p_{ac} are given in (18). For those who are not familiar with fluid formulations that contain initial pressure terms in the foregoing formulation, we note that if a full Newton solution iteration is adopted, then the initial pressures would be updated during the iteration process. On the other hand, if a modified Newton iteration is used, then the initial pressures would be from the last time step values.

The present partitioned Eq. (26) for internal and gravity waves possesses several noteworthy features:

- The present formulation embodies purely acoustic waves, purely gravity waves, their combined effects, depending on which of the stiffness terms are retained.
- All stiffness terms are quadratic in $\mathbf{u}_f$, which leads to a symmetric stiffness matrix.
- In keeping with the geometric stiffness concept employed in structural modeling of initial stresses, the present equation brings along the gravity pressure acting as an initial stress for modeling acoustic waves.
- When the acoustic pressure (p_{ac}) is sufficiently large, it acts as an initial acoustic geometric pressure. This may serve well for modeling of nonlinear waves whose group velocity is sufficiently different from the speed of fluid.
- It should be noted that the above fluid equation can account for cavitation models which can be important for containment vessels, especially carrying gaseous fluids. This can be realized by noting $p_{ac} = -\rho c^2\nabla\cdot\mathbf{u}_f$ for which $\nabla\cdot\mathbf{u}_f$ takes on the positive value instead of negative value for compression state.
- As discussed in [18], the preceding fluid displacement model may be transformed into a pressure-based model by replacing p_{ac} from the relation:

$$p_{ac} = -\rho c^2\nabla\cdot\mathbf{u}_f, \quad \text{subject to}: \mathbf{curl}(\mathbf{u}_f) = 0. \tag{27}$$

- The present formulation models the density stratification as indicated by the Väisälä-Brunt stiffness term. When there is no noticeable stratification, viz., $\rho'\approx 0$, the term can be ignored as $g^2/c^2 \approx 8.3\times10^{-4}$ for air and $g^2/c^2\approx 4.3\times10^{-5}$.

4.7. Comparison with existing formulations

In the work of Andrianarison and Ohayon [78] based on the Lighthill model of gravity and compressibility interaction contribu-

tions [75], they reported the following formulations (see Eq. (19) therein):

$$\begin{aligned}
&\text{Inertia force}: \int_{V_f} \rho_0 \ddot{\mathbf{u}} \cdot \delta \mathbf{u}_f \, dV,\\
&\text{Acoustic stiffness}: + \int_{V_f} (\nabla \cdot \mathbf{u}_f)(\rho_0 c^2)(\nabla \cdot \delta \mathbf{u}_f) \, dV,\\
&\text{Partial Väisälä-Brunt stiffness}: + \frac{1}{2} \int_{V_f} \rho_0(z)[-\rho' g] \delta(\mathbf{k} \cdot \mathbf{u}_f)]^2 \, dV,\\
&\text{Gravity gradient}: + \int_{V_f} \rho_0 \; \delta[(\mathbf{g} \cdot \mathbf{u}_f)(\nabla \cdot \mathbf{u}_f)] \, dV,\\
&\text{Surface stiffness}: + \int_{S_f} \rho_0 (\mathbf{g} \cdot \delta \mathbf{u}_f)(\mathbf{k} \cdot \delta \mathbf{u}_f) \, dS,\\
&\text{Body force}: = \int_{V_f} \mathbf{f}(t) \cdot \delta \mathbf{u}_f \, dV.
\end{aligned} \tag{28}$$

Observe that the first three terms in $(28)_{1\text{-}3}$ and the surface stiffness terms are regular and yield symmetric matrices. The gravity gradient term yields, while symmetric, rank-deficient arrow-head type matrix. In contrast, all of the terms in the present derivation(26) yield symmetric and regular matrices. In addition, the initial gravity pressure and acoustic geometric stiffness terms are absent in their formulation.

5. Variational formulation of flexible structures

In the variational formulation of internal and gravity waves carried out in the previous section, the fluid motion is assumed to be small. This means the interacting structural motion must be also small. This does not imply the structure behave linearly. In fact it would be sensible for the structure to undergo both geometric and material nonlinear states. To this end, we start the present variational formulation of the structural partition with the following virtual work for the structure:

$$\begin{aligned}
\delta \Pi_s &= \int_{V_0} \{\nabla_0 \cdot \mathbf{T} + \mathbf{b}_0 - \rho_0 \ddot{\mathbf{u}}_s\} \cdot \delta \mathbf{u}_s \, dV_0 = 0,\\
&= \int_V \{\nabla \cdot \boldsymbol{\sigma} + \mathbf{b} - \rho \ddot{\mathbf{u}}_s\} \cdot \delta \mathbf{u}_s dV = 0,\\
\nabla &= \frac{\partial}{\partial x}\mathbf{i} + \frac{\partial}{\partial x}\mathbf{j} + \frac{\partial}{\partial x}\mathbf{k}, \rho \, dV = \rho_0 \, dV_0, \quad \rho \mathbf{b} \, dV = \rho_0 \mathbf{b}_0 \, dV_0.
\end{aligned} \tag{29}$$

In the preceding equation, the first Piola–Kirchhoff stress tensor ($\mathbf{T}$), and the current position vector ($\mathbf{x}_s$), the displacement ($\mathbf{u}_s$), etc. are defined in the same way as introduced in the virtual work statement for the fluid (10). It should be noted that the above principle of virtual work satisfies the equations of motion for a continuum plus the boundary conditions:

$$\mathbf{u}_s - \bar{\mathbf{u}}_s = 0 \quad \text{on } \Gamma_u \boldsymbol{\tau}_s - \boldsymbol{\sigma} \cdot \mathbf{n}_\sigma = 0 \quad \text{on } \Gamma_\sigma \tag{30}$$

provided the virtual displacement $\delta \mathbf{u}_s$ is chosen to satisfy

$$\delta \mathbf{u}_s = 0 \quad \text{on } \Gamma_u. \tag{31}$$

In (30) the displacement $\mathbf{u}_s$ is prescribed on Γ_u and the traction $\boldsymbol{\tau}$ represents the prescribed traction on Γ_σ and $\mathbf{n}_\sigma$ is unit normal vector on the traction surface S. It should be noted that Γ_u and Γ_σ exclude the fluid–structure interface which is treated as internal constraint in the present paper.

The structural virtual work can be expressed either in the undeformed configuration$(29)_1$ or in the deformed configuration$(29)_2$, with the former leading to the total Lagrangian procedure [79–84] and the latter to the updated Lagrangian or corotational solution procedures [85–89]. In the present derivation, we will adopt the corotational formulation because of our familiarity with that kinematical description.

Integrating by parts the virtual work due to the strain energy we obtain:

$$\int_V (\nabla \cdot \boldsymbol{\sigma}) \cdot \delta \mathbf{u} \, dV = \int_{\Gamma_\sigma} \boldsymbol{\tau}_s \cdot \delta \mathbf{u}_s \, d\Gamma - \int_V \boldsymbol{\sigma} : \nabla \delta \mathbf{u}_s \, dV, \tag{32}$$

where the symmetry of the Cauchy stress tensor, viz., $\boldsymbol{\sigma}^T = \boldsymbol{\sigma}$, has been used. Substituting into $(29)_2$ leads to

$$\begin{aligned}
&\delta \boldsymbol{E}^{inertia}(\ddot{\mathbf{x}}) + \delta \boldsymbol{E}^{int}(\mathbf{x}) = \delta \boldsymbol{E}^{ext}(\mathbf{x}),\\
&\delta \boldsymbol{E}^{inertia}(\ddot{\mathbf{x}}) = \int_V \rho \ddot{\mathbf{u}}_s \cdot \delta \mathbf{u}_s \, dV,\\
&\delta \boldsymbol{E}^{int}(\mathbf{x}) = \int_V \boldsymbol{\sigma} : \nabla \delta \mathbf{u}_s \, dV,\\
&\delta \boldsymbol{E}^{ext}(\mathbf{x}) = \int_V \mathbf{b} \cdot \delta \mathbf{u}_s \, dV + \int_{\Gamma_\sigma} \boldsymbol{\tau}_s \cdot \delta \mathbf{u}_s \, d\Gamma,\\
&\mathbf{x} = \mathbf{X} + \mathbf{u}_s.
\end{aligned} \tag{33}$$

Discretization and subsequent solution of the above equation for structures require linearization of $\delta \boldsymbol{E}^{int}$. To this end, a constitutive relation based on the Truesdell stress rate [90,82] can be stated as

$$\begin{aligned}
&\triangle \boldsymbol{\sigma}^{<T>} = \triangle \boldsymbol{\sigma} - \boldsymbol{l} \cdot \sigma - \boldsymbol{\sigma} \cdot \boldsymbol{l}^T + tr(\mathbf{l})\boldsymbol{\sigma}, \quad \boldsymbol{l} = \triangle \bar{\mathbf{F}} \cdot \bar{\mathbf{F}}^{-1},\\
&\boldsymbol{e}(\triangle \mathbf{u}_s) = \frac{1}{2}\{\bar{\nabla}(\triangle \mathbf{u}_s) + \bar{\nabla}(\triangle^T \mathbf{u}_s)\},\\
&\bar{\nabla} = \frac{\partial}{\partial \bar{x}}\mathbf{i} + \frac{\partial}{\partial \bar{y}}\mathbf{j} + \frac{\partial}{\partial \bar{z}}\mathbf{k}, \quad \bar{\mathbf{x}} = \mathbf{X} + \bar{\mathbf{u}}_s,\\
&\bar{\mathbf{F}} = \mathbf{F}_{\bar{\mathbf{u}}_s},\\
&\triangle \bar{\mathbf{F}} = \bar{\nabla}(\triangle \mathbf{u}_s), \quad \mathbf{u}_s = \bar{\mathbf{u}}_s + \triangle \mathbf{u}_s.
\end{aligned} \tag{34}$$

An incremental constitutive relation we adopt may be expressed as

$$\triangle \begin{Bmatrix} \sigma_{11} \\ \sigma_{22} \\ \sigma_{33} \\ \sigma_{12} \\ \sigma_{23} \\ \sigma_{31} \end{Bmatrix} = \begin{bmatrix} c_{11} & c_{12} & c_{13} & c_{14} & c_{15} & c_{16} \\ & c_{22} & c_{23} & c_{24} & c_{25} & c_{26} \\ & & c_{33} & c_{34} & c_{35} & c_{36} \\ & & & c_{44} & c_{45} & c_{46} \\ & & & & c_{55} & c_{56} \\ sym. & & & & & c_{66} \end{bmatrix} \triangle \begin{Bmatrix} \varepsilon_{11} \\ \varepsilon_{22} \\ \varepsilon_{33} \\ \varepsilon_{12} \\ \varepsilon_{23} \\ \varepsilon_{31} \end{Bmatrix},$$

$$\varepsilon_{ij} = \frac{1}{2}\left(\frac{\partial u_i}{\partial x_j} + \frac{\partial u_j}{\partial x_i}\right). \tag{35}$$

Taking the Frechet derivative of $\delta \boldsymbol{E}^{int}$ utilizing the above constitutive relation, and after considerable algebraic manipulations, we arrive at the following linearization:

$$\begin{aligned}
&\delta \boldsymbol{E}^{int}(\bar{\mathbf{x}} + \triangle \mathbf{u}_s) = \delta \boldsymbol{E}^{int}(\bar{\mathbf{x}}) + \boldsymbol{K}(\triangle \mathbf{u}_s),\\
&\delta \boldsymbol{E}^{int}(\bar{\mathbf{x}}) = \int_{\bar{V}} \delta \boldsymbol{\varepsilon}_v^T \boldsymbol{\sigma}_v \, d\bar{V},\\
&\boldsymbol{K}(\triangle \mathbf{u}_s) = \boldsymbol{K}_{mat}(\triangle \mathbf{u}_s) + \boldsymbol{K}_{geom}(\triangle \mathbf{u}_s),\\
&\boldsymbol{K}_{mat}(\triangle \mathbf{u}_s) = \int_{\bar{V}} \delta \boldsymbol{\varepsilon}_v^T \mathbf{C}_m^{<T>} \triangle \boldsymbol{\varepsilon}_v \, d\bar{V},\\
&\boldsymbol{K}_{geom}(\triangle \mathbf{u}_s) = \int_{\bar{V}} \sum_{i=1}^{3} \bar{\nabla}(\delta u_i) \cdot \bar{\boldsymbol{\sigma}} \cdot \bar{\nabla}(\triangle u_i) \, d\bar{V}.
\end{aligned} \tag{36}$$

The linearized variational equation of motion for structures can now be written as

$$\begin{aligned}
&\delta \boldsymbol{E}^{inertia}(\triangle \ddot{\mathbf{u}}_s) + \boldsymbol{K}_{mat}(\triangle \mathbf{u}_s) + \boldsymbol{K}_{geom}(\triangle \mathbf{u}_s)\\
&\quad = \delta \boldsymbol{E}^{ext}(\mathbf{x}) - \delta \boldsymbol{E}^{inertia}(\ddot{\bar{\mathbf{x}}}_s) - \delta \boldsymbol{E}^{int}(\bar{\mathbf{x}}_s).
\end{aligned} \tag{37}$$

In the remainder of the paper we consider the structure undergoing small strains yet with finite displacements and rotations but small strains. Thus the geometric stiffness force must be retained. When this assumption is invoked, the foregoing equation simplifies to

With $\bar{\mathbf{u}}_s = 0 \quad \Rightarrow \quad \triangle\mathbf{u}_s \rightarrow \mathbf{u}_s$:

$$\Downarrow$$

$$\delta\boldsymbol{E}^{inertia}(\ddot{\mathbf{u}}_s) + \boldsymbol{K}_{mat}(\mathbf{u}_s) + \boldsymbol{K}_{geom}(\mathbf{u}_s) = \delta\boldsymbol{E}^{ext}(\mathbf{x}) \tag{38}$$

Or, expressed in terms of $\delta\Pi_s^{lin}$

$$\delta\Pi_s^{lin} = \delta\boldsymbol{E}^{ext}(\mathbf{x}) - \delta\boldsymbol{E}^{inertia}(\ddot{\mathbf{u}}_s) - \boldsymbol{K}_{mat}(\mathbf{u}_s) - \boldsymbol{K}_{geom}(\mathbf{u}_s) = 0.$$

It should be mentioned that a parallel linearization can be carried out for the use of structural analysis software that is based on the total Lagrangian formulation [79,80,90,84]. Here one replaces the linearized constitutive relation (35) by the corresponding linearized one based on the second Piola–Kirchhoff (2nd P–K) stress tensor, and similarly the initial Cauchy stress by the 2nd P–K stress tensor, respectively. One also must use the Green–Lagrange strain measures for consistency.

6. Discrete equations for coupled internal waves and structures

Discretization of both the variational fluid Eq. (26) and the variational linearized structural Eq. (38) by the finite element method is well documented (cf. Zienkiewicz [91] and Pironneau [92]). Thus we will simply state the discrete equations. Discretization of the internal fluid–structure interface, however, is not straightforward as explained next.

6.1. Discretization of interface constraint functional

A simple algorithm for discretizing the localized interface constraint collocates the localized Lagrange multipliers (λ) with the interface displacement. This means that we place a fluid-side Lagrange multiplier set(λ_f) for each interface fluid node, and similarly for each structural node (see Fig. 2). Hence, discretization of the interface constraint is reduced to determine the frame nodes and interpolate the frame elements. A more detailed procedure for determining the frame nodes may be found in [93].

For the present problem, the localized Lagrange multipliers are normal components. Hence, we sample them at the element centroids for linear or constant-strain elements, requiring only one Lagrange multiplier per elements. This is illustrated in the example problem shown in Fig. 4 For this example problem, the present localized interface constraint functional (6) is shown to be discretized as(see, for the detailed procedure, [94])

$$\begin{aligned}\pi_\ell(\mathbf{u}_f, \mathbf{u}_s, \mathbf{u}_b, \lambda_f, \lambda_s) &= \int_{S_f} \lambda_f^T(\mathbf{u}_f - \mathbf{u}_b)\cdot\mathbf{n}\,dS + \int_{S_s} \lambda_s^T(\mathbf{u}_s - \mathbf{u}_b)\\ &\quad\cdot\mathbf{n}\,dS\\ &= \begin{bmatrix}\lambda_f^T & \lambda_s^T\end{bmatrix}\left(\begin{bmatrix}\mathbf{B}_f & 0\\ 0 & \mathbf{B}_s\end{bmatrix}\begin{bmatrix}\mathbf{u}_f\\ \mathbf{u}_s\end{bmatrix} - \begin{bmatrix}\mathbf{L}_f\\ \mathbf{L}_s\end{bmatrix}\mathbf{u}_b\right).\end{aligned} \tag{39}$$

In the foregoing equation the discretized quantities referring to Fig. 4 are given by

$$\begin{aligned}&\mathbf{B}_f = \frac{1}{2}\begin{bmatrix}1 & 1 & 0\\ 0 & 1 & 1\end{bmatrix}, \quad \mathbf{B}_s = \frac{1}{2}\begin{bmatrix}1 & 1 & 0 & 0\\ 0 & 1 & 1 & 0\\ 0 & 0 & 1 & 1\end{bmatrix},\\ &\mathbf{L}_f = \frac{1}{16}\begin{bmatrix}7 & 9 & 0 & 0\\ 0 & 9 & 7 & 0\end{bmatrix}, \quad \mathbf{L}_s = \frac{1}{8}\begin{bmatrix}5 & 3 & 0 & 0\\ 0 & \frac{1}{2} & \frac{1}{2} & 0\\ 0 & 0 & 3 & 5\end{bmatrix},\\ &\boldsymbol{\lambda}_f^T = [\lambda_f^{(1)} \;\; \lambda_f^{(2)}], \quad \boldsymbol{\lambda}_s^T = [\lambda_s^{(1)} \;\; \lambda_s^{(2)} \;\; \lambda_s^{(3)}],\\ &\mathbf{u}_f^T = [u_f^{(1)} \;\; u_f^{(2)} \;\; u_f^{(3)}],\\ &\mathbf{u}_s^T = [u_s^{(1)} \;\; u_s^{(2)} \;\; u_s^{(3)} \;\; u_s^{(4)}],\\ &\mathbf{u}_b^T = [u_b^{(1)} \;\; u_b^{(2)} \;\; u_b^{(3)} \;\; u_b^{(4)}].\end{aligned} \tag{40}$$

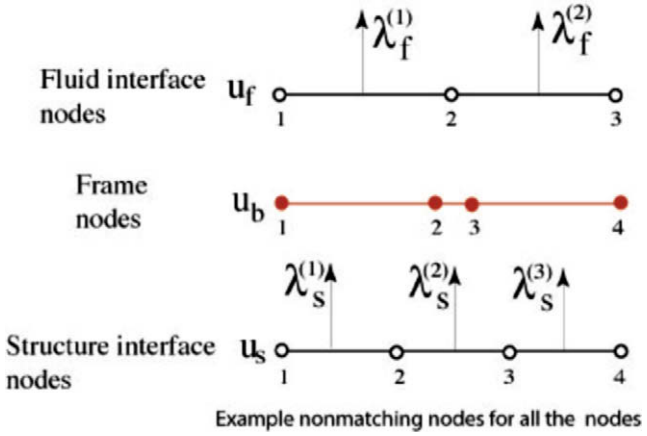

Fig. 4. Nonmatching localized interface example.

There is an important geometrical consideration that must be incorporated when the interface is curved because the normals on the fluid elements, the frame elements and the structural elements do not necessarily coincide. This is illustrated in Fig. 5. Specifically, the difference in the normals should be taken care of as shown in (41). DeRuntz and Geers [95] used a similar approach in their computation of added mass when boundary element method was used to account for the pressure acting on the structural surface via added mass modification.

$$\begin{aligned}\pi_\ell &= \sum_{i=1}^{N_f} \lambda_f^{(i)}(\mathbf{n}_f^{(i)}\cdot\mathbf{u}_f^{(i)}(0) - \mathbf{n}_f^{(i)}\cdot\mathbf{n}_b^{(i)}\mathbf{u}_b^{(i)}(\xi_f))\\ &\quad + \sum_{i=1}^{N_s} \lambda_s^{(i)}(\mathbf{n}_s^{(i)}\cdot\mathbf{u}_s^{(i)}(0) - \mathbf{n}_s^{(i)}\cdot\mathbf{n}_b^{(i)}\mathbf{u}_b^{(i)}(\xi_s))\\ &\qquad\Downarrow\\ \pi_\ell &= \boldsymbol{\lambda}_f^T(\tilde{\mathbf{B}}_f\mathbf{u}_f - \tilde{\mathbf{L}}_f\mathbf{u}_b) + \boldsymbol{\lambda}_f^T(\tilde{\mathbf{B}}_s\mathbf{u}_s - \tilde{\mathbf{L}}_s\mathbf{u}_b),\end{aligned} \tag{41}$$

where the normals and the evaluation coordinates on the frame element are shown in Fig. 5; $u(0)$ indicates that the displacements are evaluated at the element centroid; $u_b(\xi_f)$ denotes the mid-point of the interfacing fluid element mapped onto the frame element coordinates, and likewise $u_b(\xi_s)$; and (N_f, N_s) are the total number of interfacing elements for fluid and structure, respectively.

6.2. Discretization of fluid equation

Finite element discretization of the fluid equation is straightforward in that the fluid displacement $\mathbf{u}_f$ is interpolated by the stan-

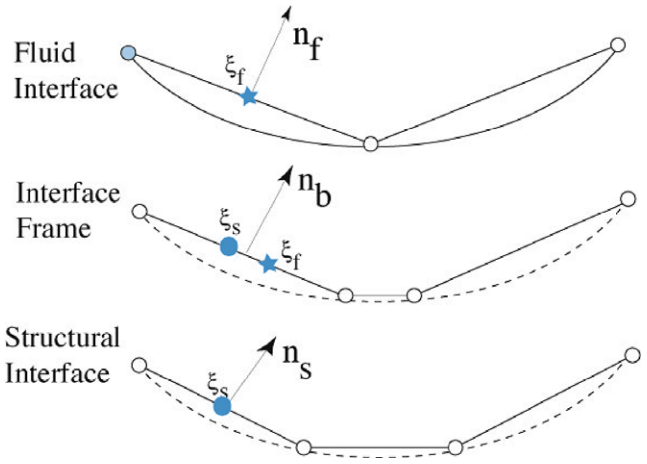

Fig. 5. Nonmatching localized interface example for curved interface.

dard isoparametric basis functions and the pressure is sampled at the Barlow points. That is, for constant-strain elements at the element centroid. The resulting discretization of the variational fluid Eq. (26) can be stated as

$$\delta\tilde{\Pi}_f = \delta\mathbf{u}_f(\mathbf{f}_f - \mathbf{M}_f\ddot{\mathbf{u}}_f - \mathbf{K}_f(\mathbf{u}_f, p_{ac}, p_{gr})\ \mathbf{u}_f) \tag{42}$$

It should be noted that the fluid stiffness matrix, $\mathbf{K}_f(\mathbf{u}_f, p_{ac}, p_{gr})$, consists of the acoustic stiffness, Väisälä-Brunt stiffness for stratifying fluids, geometric stiffness due to gravity pressure, and geometric stiffness due to acoustic pressure.

6.3. Discretization of structural equation

As stated, it is a standard practice to obtain the discrete version of the linearized variational equation for structure (38) as

$$\delta\tilde{\Pi}_s^{lin} = \delta\mathbf{u}_s(\mathbf{f}_s - \mathbf{M}_s\ddot{\mathbf{u}}_s - \mathbf{K}_s(\boldsymbol{\sigma})\ \mathbf{u}_s) \tag{43}$$

where the stiffness matrix, $\mathbf{K}(\boldsymbol{\sigma})$, consists of the material and geometric stiffness matrices as discussed in (38).

6.4. Discrete partitioned fluid–structure interaction equations

The coupled partitioned fluid–structure interaction model can now be constructed by the following variational statement:

$$\delta\Pi_{total} = \delta\pi_\ell + \delta\Pi_f + \delta\Pi_s = 0 \tag{1}$$

Inserting the discrete variational internal constraint (41), the discrete variational fluid Eq. (42) and the discrete variational structural Eq. (43) into the foregoing equation, the stationarity of the resulting expression yields the following equation set:

$$\begin{bmatrix} \mathbf{K}_f + \mathbf{M}_f\frac{d^2}{dt^2} & \mathbf{0} & \tilde{\mathbf{B}}_f^T & \mathbf{0} & \mathbf{0} \\ \mathbf{0} & \mathbf{K}_s + \mathbf{M}_s\frac{d^2}{dt^2} & \mathbf{0} & \tilde{\mathbf{B}}_s^T & \mathbf{0} \\ \tilde{\mathbf{B}}_f & \mathbf{0} & \mathbf{0} & \mathbf{0} & -\tilde{\mathbf{L}}_f \\ \mathbf{0} & \tilde{\mathbf{B}}_s & \mathbf{0} & \mathbf{0} & -\tilde{\mathbf{L}}_s \\ \mathbf{0} & \mathbf{0} & -\tilde{\mathbf{L}}_f^T & -\tilde{\mathbf{L}}_s^T & \mathbf{0} \end{bmatrix} \begin{bmatrix} \mathbf{u}_f \\ \mathbf{u}_s \\ \boldsymbol{\lambda}_f \\ \boldsymbol{\lambda}_s \\ \mathbf{u}_b \end{bmatrix} = \begin{bmatrix} \mathbf{f}_f \\ \mathbf{f}_s \\ \mathbf{0} \\ \mathbf{0} \\ \mathbf{0} \end{bmatrix} \tag{44}$$

7. Vibration and transient analysis by present partitioned fluid–structure interaction equations

Efficient algorithms exist for the transient analysis of the above partitioned multi-physics models [96,97,59,60,63] and for vibration analysis including reduced-order models [98,99]. While we defer detailed aspects of computational procedures and numerical experiments for a later exposition, we briefly discuss several special analyses that can accrue from the above formulation (44).

7.1. Vibration analysis of FSI systems

Eq. (44) can be specialized to vibration formulation by taking

$$\frac{d^2}{dt^2} = -\omega_2, \quad \text{with} \quad \mathbf{f}_s = \mathbf{f}_f = \mathbf{0} \tag{45}$$

whose substitutions leads to

$$\begin{bmatrix} \mathbf{K}_f - \omega^2\mathbf{M}_f & \mathbf{0} & \tilde{\mathbf{B}}_f^T & \mathbf{0} & \mathbf{0} \\ \mathbf{0} & \mathbf{K}_s - \omega^2\mathbf{M}_s & \mathbf{0} & \tilde{\mathbf{B}}_s^T & \mathbf{0} \\ \tilde{\mathbf{B}}_f & \mathbf{0} & \mathbf{0} & \mathbf{0} & -\tilde{\mathbf{L}}_f \\ \mathbf{0} & \tilde{\mathbf{B}}_s & \mathbf{0} & \mathbf{0} & -\tilde{\mathbf{L}}_s \\ \mathbf{0} & \mathbf{0} & -\tilde{\mathbf{L}}_f^T & -\tilde{\mathbf{L}}_s^T & \mathbf{0} \end{bmatrix} \begin{bmatrix} \mathbf{u}_f \\ \mathbf{u}_s \\ \boldsymbol{\lambda}_f \\ \boldsymbol{\lambda}_s \\ \mathbf{u}_b \end{bmatrix} = \begin{bmatrix} \mathbf{0} \\ \mathbf{0} \\ \mathbf{0} \\ \mathbf{0} \\ \mathbf{0} \end{bmatrix} \tag{46}$$

An efficient flexibility-based vibration analysis technique including substructuring that is well suited to treat the above vibration model is discussed in [98–100].

7.2. Transient analysis of FSI systems

There are three modes of transient analysis utilizing the present partitioned FSI formulation (44): explicit-explicit (meaning explicit integration for both fluid and structural partitioned equations), explicit–implicit and implicit–implicit integration. We will describe the implicit–implicit integration procedure and show that the explicit-explicit and explicit–implicit procedure follows by extrapolating the stiffness force terms. For illustration purposes, we employ the implicit-mid-point rule for both the fluid and structural equations of motion:

$$\begin{aligned} &\dot{\mathbf{u}}^{n+\frac{1}{2}} = \dot{\mathbf{u}}^n + \delta\ddot{\mathbf{u}}^{n+\frac{1}{2}}, \quad \delta = \frac{1}{2}\triangle t \\ &\mathbf{u}^{n+\frac{1}{2}} = \mathbf{u}^n + \delta\dot{\mathbf{u}}^{n+\frac{1}{2}} \\ &\qquad \Downarrow \\ &\mathbf{u}^{n+\frac{1}{2}} = \mathbf{h}_u^{n+\frac{1}{2}} + \delta^2\ddot{\mathbf{u}}^{n+\frac{1}{2}}, \quad \mathbf{h}_u^{n+\frac{1}{2}} = \mathbf{u}^n + \delta\dot{\mathbf{u}}^n \end{aligned} \tag{47}$$

where $\triangle t$ is the step size. Once $\mathbf{u}^{n+\frac{1}{2}}$ is obtained, $\mathbf{u}^{n+1}$ can be obtained from

$$\mathbf{u}^{n+1} = 2\mathbf{u}^{n+\frac{1}{2}} - \mathbf{u}^n \tag{48}$$

Substituting into (44) we obtain the following time-discretized equation:

$$\begin{aligned} &\begin{bmatrix} (\frac{1}{\delta^2}\mathbf{M}_f + \mathbf{K}_f^n) & \mathbf{0} & \tilde{\mathbf{B}}_f^T & \mathbf{0} & \mathbf{0} \\ \mathbf{0} & (\frac{1}{\delta^2}\mathbf{M}_s + \mathbf{K}_s^n) & \mathbf{0} & \tilde{\mathbf{B}}_s^T & \mathbf{0} \\ \tilde{\mathbf{B}}_f & \mathbf{0} & \mathbf{0} & \mathbf{0} & -\tilde{\mathbf{L}}_f \\ \mathbf{0} & \tilde{\mathbf{B}}_s & \mathbf{0} & \mathbf{0} & -\tilde{\mathbf{L}}_s \\ \mathbf{0} & \mathbf{0} & -\tilde{\mathbf{L}}_f^T & -\tilde{\mathbf{L}}_s^T & \mathbf{0} \end{bmatrix} \begin{bmatrix} \mathbf{u}_f \\ \mathbf{u}_s \\ \boldsymbol{\lambda}_f \\ \boldsymbol{\lambda}_s \\ \mathbf{u}_b \end{bmatrix}^{n+\frac{1}{2}} \\ &= \begin{bmatrix} \mathbf{f}_f + \frac{1}{\delta^2}\mathbf{M}_f\mathbf{h}_{u_f} \\ \mathbf{f}_s + \frac{1}{\delta^2}\mathbf{M}_s\mathbf{h}_{u_s} \\ \mathbf{0} \\ \mathbf{0} \\ \mathbf{0} \end{bmatrix}^{n+\frac{1}{2}} \end{aligned} \tag{49}$$

where the stiffness matrices $(\mathbf{K}_f, \mathbf{K}_s)$ are approximated by using the displacement, pressures and stresses at the nth step values.

The numerical solution of the above discrete equation can be effected by employing a parallel solution algorithm described in [60]. Alternatively, one may employ a more mature FETI-DP or its allied methods [62], by solving for $(\mathbf{u}_f, \mathbf{u}_s)$ first, then projecting out the frame displacement $\mathbf{u}_b$ except the so-called *cross points* interface degrees of freedom, and the localized Lagrange multipliers are transforming the present localized Lagrange multipliers to the classical *global* Lagrange multipliers as detailed in [57]. There exist a plethora of allied methods labeled as semi-implicit algorithm (see, e.g., Sy and Murea [101]) that do need to satisfy the interface compatibility constraints at each time step. This may present fruitful avenue for further study.

7.2.1. Explicit–implicit transient analysis procedure

For explicit–implicit procedure, i.e., integrating the fluid equations by an explicit integration formula and the structural equations by an implicit formula, all one needs to do is to transfer the fluid stiffness force term to the right-hand side with the displacement replaced by a predictor. This is illustrated in the equation below.

$$\begin{bmatrix} \frac{1}{\delta^2}\mathbf{M}_f & \mathbf{0} & \tilde{\mathbf{B}}_f^T & \mathbf{0} & \mathbf{0} \\ \mathbf{0} & (\frac{1}{\delta^2}\mathbf{M}_s + \mathbf{K}_s^n) & \mathbf{0} & \tilde{\mathbf{B}}_s^T & \mathbf{0} \\ \tilde{\mathbf{B}}_f & \mathbf{0} & \mathbf{0} & \mathbf{0} & -\tilde{\mathbf{L}}_f \\ \mathbf{0} & \tilde{\mathbf{B}}_s & \mathbf{0} & \mathbf{0} & -\tilde{\mathbf{L}}_s \\ \mathbf{0} & \mathbf{0} & -\tilde{\mathbf{L}}_f^T & -\tilde{\mathbf{L}}_s^T & \mathbf{0} \end{bmatrix} \begin{bmatrix} \mathbf{u}_f \\ \mathbf{u}_s \\ \lambda_f \\ \lambda_s \\ \mathbf{u}_b \end{bmatrix}^{n+\frac{1}{2}} = \begin{bmatrix} (\mathbf{f}_f - \mathbf{K}_f\mathbf{u}_f^n) + \frac{1}{\delta^2}\mathbf{M}_f\mathbf{h}_{u_f} \\ \mathbf{f}_s + \frac{1}{\delta^2}\mathbf{M}_s\mathbf{h}_{u_s} \\ \mathbf{0} \\ \mathbf{0} \\ \mathbf{0} \end{bmatrix}^{n+\frac{1}{2}} \tag{50}$$

It can be shown that the net result of the foregoing procedure is equivalent to integrating the fluid equations by the central difference formula while implicitly integrating the structural equations by the trapezoidal rule.

7.2.2. Explicit-explicit transient analysis procedure

A straightforward explicit-explicit procedure can be realized by transferring the $(\mathbf{K}_s\mathbf{u}_s^{n+\frac{1}{2}})$-term to the right-hand side with $\mathbf{u}_s^{n+\frac{1}{2}} \approx \mathbf{u}_s^n$. This is described below.

$$\begin{bmatrix} \frac{1}{\delta^2}\mathbf{M}_f & \mathbf{0} & \tilde{\mathbf{B}}_f^T & \mathbf{0} & \mathbf{0} \\ \mathbf{0} & \frac{1}{\delta^2}\mathbf{M}_s & \mathbf{0} & \tilde{\mathbf{B}}_s^T & \mathbf{0} \\ \tilde{\mathbf{B}}_f & \mathbf{0} & \mathbf{0} & \mathbf{0} & -\tilde{\mathbf{L}}_f \\ \mathbf{0} & \tilde{\mathbf{B}}_s & \mathbf{0} & \mathbf{0} & -\tilde{\mathbf{L}}_s \\ \mathbf{0} & \mathbf{0} & -\tilde{\mathbf{L}}_f^T & -\tilde{\mathbf{L}}_s^T & \mathbf{0} \end{bmatrix} \begin{bmatrix} \mathbf{u}_f \\ \mathbf{u}_s \\ \lambda_f \\ \lambda_s \\ \mathbf{u}_b \end{bmatrix}^{n+\frac{1}{2}} = \begin{bmatrix} (\mathbf{f}_f - \mathbf{K}_f\mathbf{u}_f^n) + \frac{1}{\delta^2}\mathbf{M}_f\mathbf{h}_{u_f} \\ (\mathbf{f}_s - \mathbf{K}_s\mathbf{u}_s^n) + \frac{1}{\delta^2}\mathbf{M}_s\mathbf{h}_{u_s} \\ \mathbf{0} \\ \mathbf{0} \\ \mathbf{0} \end{bmatrix}^{n+\frac{1}{2}} \tag{51}$$

In passing, it should be noted that the present partitioned FSI formulation (44) reduces to a monolithic formulation if the interface forces (λ_f, λ_s) are eliminated. While the reduction is straightforward for matching interfaces, they are not trivial for nonmatching interfaces, let alone destroying software modularity.

A computationally efficient and still adhering to partitioned solution process can be developed as follows. First, obtain $(\mathbf{u}_f^{n+\frac{1}{2}}, \mathbf{u}_f^{n+\frac{1}{2}})$ from the first two of the explicit–implicit equation set (51) and then consequently $(\mathbf{u}_f^{n+1}, \mathbf{u}_f^{n+1})$ via (48). Here we assume to have used diagonalized mass matrices.

Second, instead of implicitly solving simultaneously $(\lambda_f, \lambda_s, \mathbf{u}_b)^{n+\frac{1}{2}}$, we proceed as follows. Obtain $\mathbf{u}_b$ from a least squares solution of the third and fourth equation of (51):

$$\mathbf{u}_b^{n+1} = \begin{bmatrix} \tilde{\mathbf{L}}_f \\ \tilde{\mathbf{L}}_s \end{bmatrix}^+ \begin{bmatrix} \tilde{\mathbf{B}}_f & \mathbf{0} \\ \mathbf{0} & \tilde{\mathbf{B}}_s \end{bmatrix} \begin{bmatrix} \mathbf{u}_f \\ \mathbf{u}_s \end{bmatrix}^{n+1} \tag{52}$$

where the superscript $()^+$ denotes pseudo-inverse of a rectangular matrix.

Third, using $\mathbf{u}_b^{n+1}$ and its previous-step values, obtain $\ddot{\mathbf{u}}_b^{n+1}$.

Fourth, twice-differentiate the compatibility equations, viz., the third and fourth equation set, to obtain

$$\begin{bmatrix} \tilde{\mathbf{B}}_f & \mathbf{0} \\ \mathbf{0} & \tilde{\mathbf{B}}_s \end{bmatrix} \begin{bmatrix} \ddot{\mathbf{u}}_f \\ \ddot{\mathbf{u}}_s \end{bmatrix}^{n+1} = \begin{bmatrix} \tilde{\mathbf{L}}_f \\ \tilde{\mathbf{L}}_s \end{bmatrix} \ddot{\mathbf{u}}_b^{n+1} \tag{53}$$

Fifth, introduce from the first and second equation of (44) to express $(\ddot{\mathbf{u}}_f^{n+1}, \ddot{\mathbf{u}}_f^{n+1})$ as

$$\begin{aligned} \ddot{\mathbf{u}}_f^{n+1} &= \mathbf{M}_f^{-1}\left(\mathbf{f}_f^{n+1} - \mathbf{K}_f\mathbf{u}_f^{n+1} - \tilde{\mathbf{B}}_f\lambda_f^{n+1}\right) \\ \ddot{\mathbf{u}}_s^{n+1} &= \mathbf{M}_s^{-1}\left(\mathbf{f}_s^{n+1} - \mathbf{K}_s\mathbf{u}_s^{n+1} - \tilde{\mathbf{B}}_s\lambda_s^{n+1}\right) \end{aligned} \tag{54}$$

Substituting $(\ddot{\mathbf{u}}_f^{n+1}, \ddot{\mathbf{u}}_f^{n+1})$ in the above equation into the twice-differentiated interface compatibility Eq. (53), one obtains the localized Lagrange multipliers computed separately in their respective software modules as

$$\begin{aligned} \lambda_f^{n+1} &= [\tilde{\mathbf{B}}_f\mathbf{M}_f^{-1}\tilde{\mathbf{B}}_f^T]^{-1}\left\{\tilde{\mathbf{B}}_f\mathbf{M}_f^{-1}\left(\mathbf{f}_f^{n+1} - \mathbf{K}_f\mathbf{u}_f^{n+1}\right) - \tilde{\mathbf{L}}_f\ddot{\mathbf{u}}_b^{n+1}\right\} \\ \lambda_s^{n+1} &= [\tilde{\mathbf{B}}_s\mathbf{M}_s^{-1}\tilde{\mathbf{B}}_s^T]^{-1}\left\{\tilde{\mathbf{B}}_s\mathbf{M}_s^{-1}\left(\mathbf{f}_s^{n+1} - \mathbf{K}_s\mathbf{u}_s^{n+1}\right) - \tilde{\mathbf{L}}_s\ddot{\mathbf{u}}_b^{n+1}\right\} \end{aligned} \tag{55}$$

Now that as the solution set for the time step t^{n+1} is available, one can proceed to integrate for the next step, namely, t^{n+2}.

8. Discussions

The present paper has focused on the partitioned formulation of a class of inviscid fluid–structure interaction system that can model sloshing and acoustic waves interacting with flexible structures. The present interface model assumes no dissipation. An immediate extension may be to generalize the present internal interface model to accommodate dissipative interface [102]. A novel feature of the present fluid formulation is that the gravity pressure and nonlinear acoustic pressure terms are retained as initial stress stiffness. This may allow to model cavitation, although not explicitly specified, within the present formulation frame work, just as plasticity can be modeled into the present structural model.

The present partitioned internal fluid–structure interaction model can be coupled with the external acoustic model [40] so that the structure sandwitched between internal fluid and external acoustic fluid field can be analyzed via a three-field partitioned solution procedure.

The present model, although it is possible to include cavitation in principle, neglects explicit inclusion of cavitation phenomena [103,104] in the model. Cavitation can be an important issue for gaseous containers. Further work is needed to adequately model cavitation within the framework of the present formulation.

For a more complete analysis of sea-borne submerged and surface vehicles, the ocean waves interacting with vehicles must be brought to bear. This and other extended modeling issues are being actively pursued and will be presented in the future.

Acknowledgements

This research was supported by the WCU (World Class University) Program through the Korea Science and Engineering Foundation funded by the Ministry of Education, Science and Technology, Republic of Korea (Grant Number R31-2008-000-10045-0). We wish to acknowledge the visiting faculty appointment of K.C. Park at Conservatoire National des Arts et Métiers (CNAM, Paris) that enabled the collaborative work reported herein. J. A. González was partially supported by the project Proyectos Investigación de Excelencia 2008, Consejeria de Innovación Ciencia y Empresa, Junta de Andalucía, Spain, with contract number P08-TEP-03804.

References

[1] D.O. Lomen, Liquid Propellant Sloshing in Mobile Tanks of Arbitrary Shape, Technical Report NASA-CR-222, National Aeronautics and Space Administration, Washington, DC, 1966.
[2] P. Tong, Liquid Sloshing in an Elastic Container, Report AFOSR-66-0943, Graduate Aeronautical Labs, California Institute of Technology, Pasadena, CA, 1966.
[3] H.N. Abramson (Ed.), The Dynamic Behaviour of Liquids in Moving Containers, NASA SP-106, Scientific and Technical Information Division, National Aeronautics and Space Administration, Washington, DC, 1966.
[4] G.R. Khabbaz, Dynamic behavior of liquids in elastic tanks, AIAA J. 9 (1971) 1985–1990.
[5] G. Everstine, A symmetric potential formulation for fluid–structure interactions, J. Sound Vibr. 79 (1981) 157–160.
[6] R. Ohayon, R. Valid, The true symmetric variational formulations for fluid–structure interaction in bounded domains-finite element results, in: R.W. Lewis, P. Bettess, E. Hinton (Eds.), Numerical Methods in Coupled Systems, Wiley, Chichester, 1984, pp. 293–326.

[7] C.A. Felippa, Symmetrization of the contained compressible fluid vibration eigenproblem, Commun. Appl. Numer. Meth. 1 (1985) 241–247.
[8] G. Sandberg, P. Göransson, A symmetric finite element formulation for acoustic fluid–structure interaction analysis, J. Sound Vibr. 123 (1988) 507–515.
[9] H.C. Chen, R.L. Taylor, Vibration analysis of fluid-solid systems using a finite element displacement formulation, Int. J. Numer. Meth. Engrg. 29 (1990) 683–698.
[10] C.A. Felippa, R. Ohayon, Mixed variational formulation of finite element analysis of acoustoelastic/slosh fluid–structure interactions, J. Fluids Struct. 4 (1990) 35–57.
[11] R. Ohayon, C.A. Felippa, The effect of wall motion on the governing equations of contained fluids, J. Appl. Mech. 57 (1990) 782–784.
[12] E. Kock, L. Olson, Fluid–structure interaction analysis by the finite-element method – a variational approach, Int. J. Numer. Meth. Engrg. 31 (1993) 463–491.
[13] H.J.P. Morand, R. Ohayon, Fluid Structure Interaction, Wiley, New York, 1995.
[14] H.F. Bauer, W. Eidel, Frictionless liquid sloshing in circular cylindrical container configurations, Aerospace Sci. Technol. 5 (1999) 301–311.
[15] A. Bermúdez, R. Rodriguez, Finite element analysis of sloshing and hydroelastic vibrations under gravity, Math. Modell. Numer. Anal. 33 (1999) 305–327.
[16] J.-S. Schotté, R. Ohayon, Effect of gravity on a free-free elastic tank partially filled with incompressible liquid, J. Fluids Struct. 18 (2003) 215–226.
[17] R.A. Ibrahim, Liquid Sloshing Dynamics: Theory and Applications, Cambridge University Press, 2005.
[18] K.C. Park, C.A. Felippa, R. Ohayon, Partitioned formulation of internal fluid–structure interaction problems by localized Lagrange multipliers, Comput. Meth. Appl. Mech. Engrg. 190 (2001) 2989–3007.
[19] P. Le Tallec, J. Mouro, Fluid–structure interaction with large structural displacements, Comput. Meth. Appl. Mech. Engrg. 190 (2001) 3039–3067.
[20] G. Sandberg, P. Goransson, A symmetric finite element formulation for acoustic fluid–structure interaction analysis, J. Sound Vibr. 123 (1988) 507–515.
[21] U. Kuttler, C. Forster, W.A. Wall, A solution for the incompressibility dilemma in partitioned fluid–structure interaction with pure Dirichlet fluid domains, Comput. Mech. 38 (2006) 417–426.
[22] J.S. Schotté, R. Ohayon, Various modelling levels to represent internal liquid behaviour in the vibration analysis of complex structures, Comput. Meth. Appl. Mech. Engrg. 198 (2009) 1913–1925.
[23] R.D. Mindlin, H.H. Bleich, Response of an elastic cylindrical shell to a transverse step shock wave, J. Appl. Mech. 20 (1953) 189–195.
[24] P. Mann-Nachbar, The interaction of an acoustic wave and an elastic spherical shell, Quart. Appl. Math. 15 (1957) 83–93.
[25] M.C. Junger, Normal modes of submerged plates and shells in fluid–solid interaction, in: J.E. Greenspon (Ed.), Proceedings of the ASME Symposium on Fluid–Structure Interaction, American Society of Mechanical Engineers, New York, 1967.
[26] H. Huang, Transient interaction of plane acoustic waves with a spherical elastic shell, J. Acoust. Soc. Am. 45 (1969) 661–670.
[27] O.C. Zienkiewicz, R.E. Newton, Coupled vibrations of a structure submerged in a compressible fluid, in: Proceedings of the International Ship Structure Congress – Symposium on the FEM Technique, Stuttgart, 1969.
[28] H.H. Bleich, I.S. Sandler, Interaction between structures and bilinear fluids, Int. J. Solids Struct. 6 (1970) 617–639.
[29] T.L. Geers, Residual potential and approximate methods for three-dimensional fluid–structure interaction problems, J. Acoust. Soc. Am. 49 (1971) 1505–1510.
[30] M.C. Junger, D. Feit, Sound, Structures and Their Interaction, MIT Press, Cambridge, MA, 1972.
[31] T.L. Geers, Doubly asymptotic approximations for transient motions of submerged structures, J. Acoust. Soc. Am. 64 (1978) 1500–1508.
[32] O.C. Zienkiewicz, P. Bettess, Fluid–structure dynamic interaction and wave forces. An introduction to numerical treatment, Int. J. Numer. Meth. Engrg. 13 (1978) 1–16.
[33] C.A. Felippa, A family of early time approximations for fluid–structure interaction, J. Appl. Mech. 47 (1980) 703–708.
[34] T.L. Geers, C.A. Felippa, Doubly asymptotic approximations for vibration analysis of submerged structures, J. Acoust. Soc. Am. 173 (1983) 1152–1159.
[35] P. Zhang, T.L. Geers, Excitation of a fluid-filled, submerged spherical shell by a transient acoustic wave, J. Acoust. Soc. Am. 93 (1993) 696–705.
[36] T.L. Geers, P. Zhang, Doubly asymptotic approximations for submerged structures with internal fluid volumes: formulation, J. Appl. Mech. 61 (1994) 893–899.
[37] R.J. Astley, Infinite elements for wave problems: a review of current formulations and an assessment of accuracy, Int. J. Numer. Meth. Engrg. 49 (2000) 951–976.
[38] S.R. Idelsohn, E. Oñate, F. del Pin, A Lagrangian meshless finite element method applied to fluid–structure interaction problems, Comput. Struct. 81 (2003) 655–671.
[39] S.R. Idelsohn, E. Oñate, F. del Pin, N. Calvo, Fluid–structure interaction using the particle finite element method, Comput. Meth. Appl. Mech. Engrg. 195 (2006) 2100–2123.
[40] M.S. Lee, Y.S. Park, Y.J. Park, K.C. Park, New approximations of external acoustic–structural interactions: derivation and evaluation, Comput. Meth. Appl. Mech. Engrg. 198 (2009) 1368–1388.
[41] C.A. Taylor, T.J.R. Hughes, C.K. Zarins, Finite element modeling of blood flow in arteries, Comput. Meth. Appl. Mech. Engrg. 158 (1998) 155–196.
[42] N. Shahcheraghi, H.A. Dwyer, A.Y. Cheer, A.I. Barakat, T. Rutaganira, Unsteady and three-dimensional simulation of blood flow in the human aortic arch, J. Biomech. Eng. 124 (2002) 378–387.
[43] M.S. Olufsen, C.S. Peskin, W.Y. Kim, E.M. Pedersen, A. Nadim, J. Larsen, Numerical simulation and experimental validation of blood flow in arteries with structured-tree outflow conditions, Ann. Biomed. Eng. 28 (2000) 1281–1299.
[44] L.Morris.P. Delassus, A. Callanan, M. Walsh, 3D numerical simulation of blood flow through models of the human aorta, J. Biomech. Eng. 127 (2005) 767–775.
[45] D.N. Ku, Blood flow in arteries, Ann. Rev. Fluid Mech. 29 (1997) 399–434.
[46] A. Quarteroni, A. Veneziani, P. Zunino, Mathematical and numerical modeling of solute dynamics in blood flow and arterial walls, SIAM J. Numer. Anal. 39 (2001) 1488–1511.
[47] E.H. Dowell, K.C. Hall, Modeling of fluid–structure interaction, Ann. Rev. Fluid Mech. 33 (2001) 445–490.
[48] A.S. Tijsseling, Fluid–structure interaction in liquid-filled pipe systems: a review, J. Fluids Struct. 10 (2) (1996) 109–146.
[49] A. de Boera, A.H. van Zuijlen, H. Biji, Review of coupling methods for nonmatching meshes, Comput. Meth. Appl. Mech. Engrg. 196 (8) (2007) 1515–1525.
[50] K.C. Park, C.A. Felippa, J.A. DeRuntz, Stabilization of staggered solution procedures for fluid–structure interaction analysis, in: T. Belytschko, T.L. Geers (Eds.), Computational Methods for Fluid Structure–Interaction Problems, vol. 26, ASME Applied Mechanics Symposia, 1977, pp. 95–124.
[51] M.A. Hamdi, Y. Ousset, G. Verchery, A displacement method for the analysis of vibrations of coupled fluid–structure systems, Int. J. Numer. Meth. Engrg. 13 (1978) 139–150.
[52] C.A. Felippa, K.C. Park, Staggered transient analysis procedures for coupled-field mechanical systems: formulation, Comput. Meth. Appl. Mech. Engrg. 24 (1980) 61–111.
[53] K.C. Park, C.A. Felippa, Partitioned analysis of coupled systems, in: T. Belytschko, T.J.R. Hughes (Eds.), Computational Methods for Transient Analysis, North-Holland, Amsterdam, New York, 1983, pp. 157–220.
[54] C.A. Felippa, J.A. DeRuntz, Finite element analysis of shock-induced hull cavitation, Comput. Meth. Appl. Mech. Engrg. 44 (1984) 297–337.
[55] A. Bermúdez, R. Rodriguez, Finite element computation of the vibration modes of a fluid-solid system, Comput. Meth. Appl. Mech. Engrg. 119 (1994) 355–370.
[56] R. Löhner, C. Yang, J. Cebral, J.D. Baum, H. Luo, D. Pelessone, C. Charman, Fluid–Structure Interaction Using a Loose Coupling Algorithm and Adaptive Unstructured Grids, AIAA-95-2259, 1995.
[57] K.C. Park, C.A. Felippa, A variational framework for solution method developments in structural mechanics, J. Appl. Mech. 65 (1998) 242–249.
[58] K.C. Park, C.A. Felippa, A variational principle for the formulation of partitioned structural systems, Int. J. Numer. Meth. Engrg. 47 (2000) 395–418.
[59] K.C. Park, U. Gumaste, C.A. Felippa, A localized version of the method of Lagrange multipliers and its applications, Comput. Mech. 24 (2000) 476–490.
[60] U. Gumaste, K.C. Park, K.F. Alvin, A family of implicit partitioned time integration algorithms for parallel analysis of heterogeneous structural systems, Comput. Mech. 24 (2000) 463–475.
[61] F.P.T. Baaijens, A fictitious domain/mortar element method for fluid–structure interaction, Int. J. Numer. Meth. Fluids 35 (7) (2001) 743–761.
[62] C. Farhat, M. Lesoinne, P. LeTallec, K. Pierson, D. Rixen, FETI-DP: a dual-primal unified FETI method: I. A faster alternative to the two-level FETI method, Int. J. Numer. Meth. Engrg. 50 (2001) 1523–1544.
[63] C.A. Felippa, K.C. Park, C. Farhat, Partitioned analysis of coupled systems, Comput. Meth. Appl. Mech. Engrg. 190 (2001) 3247–3270.
[64] W.G. Dettmer, D. Peric, A computational framework for free surface fluid flows accounting for surface tension, Comput. Meth. Appl. Mech. Engrg. 195 (2006) 3038–3071.
[65] W.A. Wall, S. Genkinger, E. Ramm, A strong coupling partitioned approach for fluid–structure interaction with free surfaces, Comput. Fluids 36 (1) (2007) 169–183.
[66] A. Legay, J. Chessa, T. Belytschko, An Eulerian–Lagrangian method for fluid–structure interaction based on level sets, Comput. Meth. Appl. Mech. Engrg. 195 (2006) 2070–2087.
[67] W.G. Dettmer, D. Peric, A fully implicit computational strategy for strongly coupled fluid–solid interaction, Arch. Comput. Meth. Engrg. 14 (2007) 205–247.
[68] C.A. Felippa, K.C. Park, Model-based partitioned analysis of coupled problems, in: G. Sandberg, R. Ohayon (Eds.), Computational Aspects of Structural Dynamics and Vibrations, CISM Courses and Lectures, vol. 505, Springer-Verlag, Berlin, 2008, pp. 171–216.
[69] M. Ross, C.A. Felippa, K.C. Park, M.A. Sprague, Treatment of acoustic fluid–structure interaction by localized Lagrange multipliers: formulation, Comput. Meth. Appl. Mech. Engrg. 197 (2008) 3057–3079.
[70] M. Ross, M.A. Sprague, C.A. Felippa, K.C. Park, Treatment of acoustic fluid–structure interaction by localized Lagrange multipliers and comparison to alternative interface coupling methods, Comput. Meth. Appl. Mech. Engrg. 197 (33–40) (2009) 3057–3079.
[71] S. Piperno, C. Farhat, Partitioned procedures for the transient solution of coupled aeroelastic problems – Part II: energy transfer analysis and three-

dimensional applications, Comput. Meth. Appl. Mech. Engrg. 190 (2001) 3147–3170.
[72] J.W.S. (Lord) Rayleigh, The Theory of Sound. Revised Edition, vol. 2, Dover, New York, 1945.
[73] H. Lamb, Hydrodynamics, sixth ed., Dover, New York, 1932.
[74] L.D. Landau, E.M. Lifshitz, Fluid Mechanics, Pergamon Press, 1959.
[75] J. Lighthill, Waves in Fluids, Cambridge University Press, 1978.
[76] G.K. Batchelor, An Introduction to Fluid Mechanics, Cambridge University Press, 1967.
[77] O. Andrianarison, R. Ohayon, Compressibility and gravity effects in internal fluid–structure vibrations: basic equations and appropriate variational formulations, Comput. Meth. Appl. Mech. Engrg. 195 (2006) 1958–1972.
[78] O. Andrianarison, R. Ohayon, Reduced models for modal analysis of fluid–structure systems taking into account compressibility and gravity effects, Comput. Meth. Appl. Mech. Engrg. 195 (2006) 5656–5672.
[79] R.H. Mallet, P.V. Marcal, Finite element analysis of nonlinear structures, J. Str. Div. ASCE 94 (1968) 2081–2105.
[80] K.-J. Bathe, E. Ramm, E.L. Wilson, Finite element formulations for large deformation dynamic analysis, Int. J. Numer. Meth. Engrg. 7 (1973) 255–271.
[81] T.J.R. Hughes, W.-K. Liu, Nonlinear finite element analysis of shells: Part I. Three-dimensional shells, Comput. Meth. Appl. Mech. Engrg. 26 (1981) 331–362.
[82] G.M. Stanley, Continuum-based Shell Elements, Ph.D. Thesis, Department of Mechanical Engineering, Stanford University, 1985.
[83] J.C. Simo, L. Vu-Quoc, A finite strain beam formulation. Part II: computational aspects, Comput. Meth. Appl. Mech. Engrg. 58 (1986) 79–116.
[84] L.A. Crivelli, C.A. Felippa, A total Lagrangian geometrically nonlinear beam element for analysis of three-dimensional space structures, Int. J. Numer. Meth. Engrg. 31 (1993) 1122–1144.
[85] O.C. Zienkiewicz, Incremental displacement in nonlinear analysis, Int. J. Numer. Meth. Engrg. 3 (1971) 387–392.
[86] T. Belytschko, B.J. Hsieh, Nonlinear transient finite element analysis with convected coordinates, Int. J. Numer. Meth. Engrg. 7 (1973) 255–271.
[87] B. Nour-Omid, C.C. Rankin, Finite rotation analysis and consistent linearization using projectors, Comput. Meth. Appl. Mech. Engrg. 93 (1991) 353–384.
[88] M.A. Crisfield, G.F. Moita, A unified co-rotational framework for solids, shells and beams, Int. J. Solids Struct. 33 (1996) 2969–2992.
[89] C.A. Felippa, B. Haugen, A unified formulation of small-strain corotational finite elements: I, Theory Comput. Meth. Appl. Mech. Engrg. 194 (2005) 2285–2336.
[90] Y.C. Fung, P. Tong, Classical and Computational Solid Mechanics, World Scientific, New Jersey, 2001.
[91] O.C. Zienkiewicz, The Finite Element Method in Engineering Science, second ed., McGraw-Hill, 1971.
[92] O. Pironneau, Finite Element Methods for Fluids, Wiley, 1989.
[93] K.C. Park, C.A. Felippa, G. Rebel, A simple algorithm for localized construction of non-matching structural interfaces, Int. J. Numer. Meth. Engrg. 53 (2002) 2117–2142.
[94] K.C. Park, C.A. Felippa, G. Rebel, Interfacing non-matching FEM meshes: the zero moment rule, in: W.A. Wall, K.-U. Bletzinger, K. Schweizerhof (Eds.), Trends in Computational Structural Mechanics, CIMNE, Barcelona, Spain, 2001, pp. 355–367.
[95] J.A. DeRuntz, T.L. Geers, Added mass computation by the boundary integral method, Int. J. Numer. Meth. Engrg. 12 (1977) 531–550.
[96] K.C. Park, M.R. Justino Jr., C.A. Felippa, An algebraically partitioned FETI method for parallel structural analysis: algorithm description, Int. J. Numer. Meth. Engrg. 40 (1997) 2717–2737.
[97] M.R. Justino Jr., K.C. Park, C.A. Felippa, An algebraically partitioned FETI method for parallel structural analysis: implementation and numerical performance evaluation, Int. J. Numer. Meth. Engrg. 40 (1997) 2739–2758.
[98] K.C. Park, Y.H. Park, Partitioned component mode synthesis via a flexibility approach, AIAA J. 42 (2004) 1236–1245.
[99] D. Markovic, K.C. Park, Reduction of substructural interface degrees of freedom in flexibility-based component mode synthesis, Int. J. Numer. Meth. Engrg. 70 (2007) 163–180.
[100] D. Markovic, A. Ibrahimbegovic, K.C. Park, Partitioning based reduced order modelling approach for transient analyses of large structures, Engrg. Comput. 26 (2009) 46–68.
[101] S. Sy, C.M. Murea, A stable time advancing scheme for solving fluid–structure interaction problem at small structural displacements, Comput. Meth. Appl. Mech. Engrg. 198 (2) (2008) 210–222.
[102] J.F. deu, W. Larbia, R. Ohayon, Vibration and transient response of structural-acoustic interior problems with dissipative interface, Comput. Meth. Appl. Mech. Engrg. 197 (51–52) (2008) 4894–4905.
[103] F.R. Young, Cavitation, McGraw-Hill Book, Co., New York, 1989.
[104] J.-P. Franc, J.-M. Michel, Fundamentals of Cavitation, Springer, Heidelberg, Germany, 2004.